Enzyme Sensing Using 2-Mercaptopyridine-Carbonitrile Reporters and Surface-Enhanced Raman Scattering

Janeala J. Morsby, Rebekah L. Thimes, Jacob E. Olson, Hannah H. McGarraugh, Jason N. Payne, Jon P. Camden,* and Bradley D. Smith*

Read Online

ACCESS | Metrics & More | Article Recommendations | Supporting Information

ABSTRACT: The high sensitivity and functional group selectivity of surface-enhanced Raman scattering (SERS) make it an attractive method for enzyme sensing, but there is currently a severe lack of enzyme substrates that release SERS reporter molecules with favorable detection properties. We find that 2-mercaptopyridine-3-carbonitrile (*o*-MPN) and 2-mercaptopyridine-5-carbonitrile (*p*-MPN) are highly effective as SERS reporter molecules that can be captured by silver or gold nanoparticles to give intense SERS spectra, each with a distinctive nitrile peak at 2230 cm^{-1}. *p*-MPN is a more sensitive reporter and can be detected at low nanomolar concentrations. An assay validation study synthesized two novel substrate molecules, **Glc-*o*-MPN** and **Glc-*p*-MPN**, and showed that they can be cleaved efficiently by β-glucosidase (K_m = 228 and 162 μM, respectively), an enzyme with broad industrial and biomedical utility. Moreover, SERS detection of the released reporters (*o*-MPN or *p*-MPN) enabled sensing of β-glucosidase activity and β-glucosidase inhibition. Comparative experiments using a crude almond flour extract showed that the presence of β-glucosidase activity could be confirmed by SERS detection in a much shorter time period (>10 time shorter) than by UV−vis absorption detection. It is likely that a wide range of enzyme assays and diagnostic tests can be developed using 2-mercaptopyridine-carbonitriles as SERS reporter molecules.
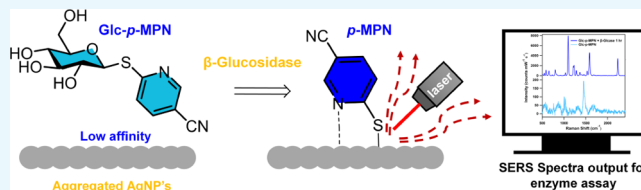
INTRODUCTION

Enzyme assays are ubiquitous in biomedical research, clinical diagnostics, drug discovery, and environmental monitoring.[1−3] The range of assay designs and experimental conditions continues to expand, creating an ongoing need to develop new ways of detecting enzymes and evaluating enzyme inhibition. Classic enzyme assays use optical techniques to monitor changes in color,[4] electronic absorption,[5] fluorescence,[6] or chemiluminescence.[7] While these methods are broadly useful, they have application-specific drawbacks such as insensitivity, background interference, high cost, or long preparation time.[8,9] These technical concerns have been motivating research efforts to develop enzyme assays with alternative detection strategies.[10,11] Advances in nanotechnology have led to new classes of nanoparticles with plasmonic properties that have great promise for exploitation within next-generation enzyme assays.[12,13] Surface-enhanced Raman scattering (SERS) is attracting a lot of attention because of its high sensitivity and functional group selectivity.[14−16] In principle, SERS is capable of enhancing the Raman scattering of the reporter molecules adsorbed on rough metallic surfaces by a factor of ∼10^6–10^{10}.[17,18] The metallic surface is often in the form of silver nanoparticles (AgNPs) or gold nanoparticles (AuNPs), which are easily prepared as monodispersed suspensions or aggregated clusters.[19]

Although the idea of incorporating SERS detection into bioanalytical methods, including enzyme assays, has been discussed for two or more decades,[17,20−22] there has been a limited applied impact. A major roadblock slowing the development of effective SERS enzyme assays is the challenge of designing suitable enzyme substrate molecules with a favorable combination of properties, including (a) rapid and selective cleavage by a target enzyme and (b) release of a reporter molecule that can be captured by AgNPs and made to elicit a large SERS response.[23] To date, only a few enzyme substrates have been reported based on a small number of releasable SERS reporter molecules such as azo, coumarin, or naphthol dyes.[17,24,25] We decided to expand the structural scope in a new direction and develop a novel set of versatile SERS reporter molecules. We were drawn to the possibility of enzyme substrates that release derivatives of 2-mercaptopyridine, which are known to have very high affinity for AgNPs and produce distinctive SERS spectral patterns.[26−30] However, there was very little literature precedence indicating if, and how, an enzyme substrate could be designed to release a suitable 2-mercaptopyridine derivative for SERS detection.

Here, we report two modified versions of 2-mercaptopyridine as highly effective SERS reporters that are captured by AgNPs with very high affinity. The compounds include a nitrile group whose vibrational stretching band is readily apparent at 2230 cm^{-1} within the open window that has very little interference from other vibrational bands (Scheme 1a).[23]

Scheme 1. (a) Capture of 2-Mercaptopyridine-carbonitrile Reporter Molecules by Aggregated AgNPs (or AuNPs) Enables Detection Using SERS and (b) Structure and Enzymatic Cleavage of the Substrates Glc-o-MPN or Glc-p-MPN by the β-Glucosidase Enzyme Gives the SERS-Active Reporter Molecules o-MPN or p-MPN, Respectively
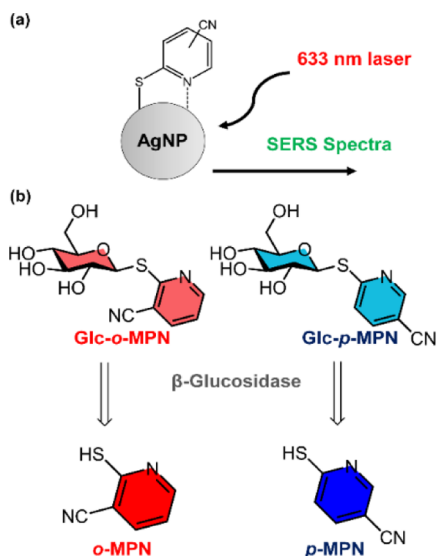
Moreover, we describe a protype SERS-active enzyme assay, which compares enzymatic cleavage of two new substrates, (2-mercaptopyridine-3-carbonitrile β-D-glucoside) (**Glc-o-MPN**) and 2-mercaptopyridine-5-carbonitrile β-D-glucoside (**Glc-p-MPN**), by the enzyme β-glucosidase (β-Glcase), to give the SERS reporters **o-MPN** and **p-MPN**, respectively (Scheme 1b). We chose to focus on β-Glcase sensing for several related reasons. It is an industrially important enzyme that is distributed widely throughout the biosphere,[31] and it is employed extensively in the industry for production of food and biofuels.[32−34] It is also a biomarker for several different diseases that require new classes of β-Glcase sensors.[35,36] From a technical perspective, β-Glcase is a good choice for early-stage, validation studies because it commercially available and its substrate selectivity profile is well-defined with reliable benchmark kinetic data (Table S1). We find that **Glc-o-MPN** and **Glc-p-MPN** are both excellent substrates for the β-Glcase enzyme, although cleavage of **Glc-p-MPN** produces a more intense SERS spectrum. The results lead us to infer that **o-MPN** or **p-MPN** can be broadly applied as reporter molecules for many bioanalytical applications using SERS detection.

■ EXPERIMENTAL SECTION

Synthesis and Characterization of SERS Substrates. Substrate synthesis and compound characterization are described in the Supporting Information. In short, **Glc-o-MPN** was synthesized in 98% yield through a modified Koenig−Knorr glycosidation between 2,3,4,6-tetra-o-acetyl-α-D-glucopyranose bromide and 2-mercaptopyridine-3-carbon-

itrile (**o-MPN**) using 2 molar equivalents of cesium carbonate in acetonitrile. The acetylated intermediate was purified by column chromatography (silica gel) and then deacetylated using aqueous triethylamine to produce **Glc-o-MPN** in 89% yield. The substrate **Glc-p-MPN** (2-mercaptopyridine-5-carbonitrile β-D-glucoside) was synthesized in one step by conducting a nucleophilic aromatic substitution reaction. Equimolar equivalents of 1-thio-β-D-glucose sodium salt and 2-chloro-5-cyanopyridine were stirred overnight in methanol to produce **Glc-p-MPN** in 38% yield after purification by column chromatography. Chemical stability studies revealed that stock supplies of **Glc-o-MPN** and **Glc-p-MPN** are highly stable when stored as dry powders (Figure S2).

Enzyme Studies Using UV−Vis Absorption. Stock solutions of 1 mM **Glc-o-MPN** and **Glc-p-MPN** were prepared in distilled water and used within a few hours. A 1 mg/mL stock solution of commercial β-glucosidase (purchased from Sigma who derived it from almonds) was prepared in 1X PBS buffer, pH 5.33, and stored at 2−8 °C. An aliquot of **Glc-o-MPN** (50 μM) and **Glc-p-MPN** was added in a cuvette containing 1× PBS buffer, pH 5.33, followed by the addition of 200 μg/mL β-glucosidase. The final 1 mL reaction mixture was mixed by inversion five times before monitoring the change in the absorption spectra over an hour. Enzyme inhibition studies were also performed using castanospermine (CAT) (10 μg/mL), a plant alkaloid inhibitor of β-glucosidase (purchased from Sigma). The order of addition was **Glc-o-MPN** or **Glc-p-MPN** (50 μM), CAT (10 μg/mL), and β-glucosidase (200 μg/mL). The Michaelis−Menten kinetic parameters were determined in 1× PBS buffer, pH 5.33, at room temperature by varying the concentration of **Glc-o-MPN** (10−500 μM) or **Glc-p-MPN** (5−200 μM) in the reaction solutions. β-Glucosidase (100 μg/mL) was added to each reaction, and the change in absorption at 300 nm for the appearance of **o-MPN** and 312 nm for the appearance of **p-MPN** was measured at 5 min intervals over an hour. A Lineweaver−Burk plot was created, and the Michaelis−Menten constant (K_m) and maximum rate (V_{max}) were calculated.

Synthesis and Characterization of Silver (Ag) Nanoparticles. AgNPs were prepared using the Lee and Meisel method.[37] Briefly, 91 mg of silver nitrate in 500 mL of water was brought to boiling under continuous stirring. Then, 10 mL of 1% (w/v) sodium citrate was added dropwise and boiled with stirring for 30 min. Upon cooling to room temperature, the colloidal dispersion was diluted to 1 L. Transmission electron microscopy (TEM) analysis of the AgNPs revealed an average particle diameter of roughly 50 nm, and UV−vis absorption showed λ_{max} = 405 nm (Figure S6).

Synthesis and Characterization of Gold (Au) Nanoparticles. Quasispherical AuNPs were synthesized according to a modified Frens method.[38] Briefly, 180 mL of 10^{-2}% (by wt) tetrachloroaurate trihydrate salt solution was brought to boiling. Then, 1.2 mL of 1% (by wt) trisodium citrate was added rapidly under vigorous stirring. Boiling was continued for 30 min before the deep red suspension with hues of yellow was allowed to cool to room temperature. SEM analysis of the AuNPs revealed an average particle diameter of 60 nm, and UV−vis absorption showed λ = 540 nm (Figure S12).

Enzyme Studies Using SERS. For all SERS studies involving AgNPs, an aliquot of **Glc-o-MPN** or **Glc-p-MPN** (10 μM) was added to a 1 mL vial containing preaggregated AgNPs (monodisperse NPs aggregated by addition of 1 M NaBr) and 1× PBS buffer, pH 5.33, followed by addition of β-
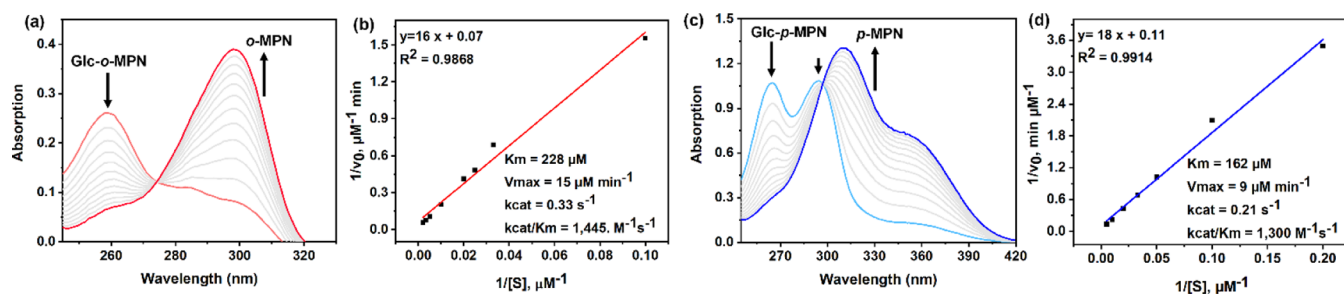
Figure 1. Representative UV−vis absorption spectra and Lineweaver Burk plots for solutions containing 50 μM **Glc-*o*-MPN** or **Glc-*p*-MPN** + 100 μg/mL β-glucosidase (β-Glcase) over a one-hour period in 1× PBS Buffer pH 5.33. (a,b) **Glc-*o*-MPN** and (c,d) **Glc-*p*-MPN**.

Glcase (200 μg/mL). For the enzyme inhibition studies, CAT (5 μg/mL) was added prior to the addition of β-Glcase. SERS spectra were measured with a custom-built Raman setup using a 633 nm HeNe laser (Thor Labs). The laser was focused onto the sample using an inverted microscope objective (Nikon, 20×, NA = 0.5) with 120 μW power, measured at the sample. The backscattered radiation was passed through a Rayleigh rejection filter (Semrock) and then dispersed with a spectrometer (Princeton Instruments Acton SP2300, grating = 600 g/mm). Light was detected using a back-illuminated, deep depletion CCD camera (PIXIS, Spec-10, Princeton Instruments) and recorded using Winspec32 software (Princeton Instruments) with a typical acquisition time of 60 s. All experiments were conducted in triplicate.

The studies that compared UV−vis and SERS detection (Figure 5) used the following conditions. The UV−vis assay tracked the changes in the spectral profile for a single 1 mL solution of **Glc-*p*-MPN** (50 μM) + almond flour extract (protein concentration of 200 μg/mL) in 1× PBS buffer, pH 5.33. The SERS assay employed a 2 mL solution of **Glc-*p*-MPN** (10 μM) + almond flour extract (protein concentration of 200 μg/mL) in buffer and removed a 1 mL aliquot at two incubation time points (1 and 24 h). Each 1 mL aliquot was added to a vial containing preaggregated AuNPs (preaggregated by addition of 1 M NaBr solution to monodisperse AuNPs), and the SERS spectrum was acquired.

Almond Flour Extract. Food-grade almond flour was purchased from a local baker and washed three times with ethyl acetate and two times with acetone to remove lipids and water. The powder was then dried immediately in a vacuum desiccator and stored at 4 °C. Afterward, 1 g of defatted flour was added to 25 mL of PBS (50 mM, pH 7.0). The supernatant (crude almond flour extract) was collected after centrifugation (room temperature, 4.4 rpm, 15 min). A Bradford assay was performed using BSA as a standard to determine the protein concentration in the crude extract (Figure S14), and a sample of the crude extract solution with a protein concentration of 200 μg/mL was subsequently tested, by UV−vis or SERS assay, for the capacity to cleave **Glc-*p*-MPN** (β-Glcase activity).[39]

RESULTS AND DISCUSSION

The results of UV−vis absorption assays (Figure 1) show that β-Glcase catalyzes the cleavage of **Glc-*o*-MPN** or **Glc-*p*-MPN**, releasing **o-MPN** or **p-MPN**, respectively, which has red-shifted absorption bands. In the case of **Glc-*p*-MPN**, the cleavage reaction was confirmed by thin-layer chromatography analysis of the assay solution (Figure S3). Enzyme inhibition studies were performed to confirm that the enzyme is

responsible for the substrate cleavage. As shown by the UV−vis spectra in Figure S5, addition of the known β-Glcase inhibitor CAT to a solution containing **Glc-*o*-MPN** or **Glc-*p*-MPN** followed by addition of the enzyme greatly slowed the appearance of absorption bands corresponding to the cleavage products, **o-MPN** or **p-MPN**.

Enzyme efficiency was quantified by conducting a series of kinetic assays that determined the Michaelis−Menten kinetics for both substrates (Figure S4). The measured values of K_m and V_{max} for **Glc-*o*-MPN** and **Glc-*p*-MPN** are similar to the values reported in the literature for other β-Glcase substrates (Table S1). The K_m for **Glc-*o*-MPN** (228 μM) was slightly higher than the K_m for **Glc-*p*-MPN** (162 μM), but **Glc-*o*-MPN** exhibited a slightly higher turnover number and catalytic efficiency (k_{cat} = 0.33 s^{-1} and k_{cat}/K_m = 1445 M^{-1} s^{-1}) than **Glc-*p*-MPN** (k_{cat} = 0.21 s^{-1} and k_{cat}/K_m = 1300 M^{-1} s^{-1}). Combined, these results indicate that **Glc-*p*-MPN** has a slightly higher affinity for the active site of the β-Glcase enzyme; however, the enzyme active site can more efficiently convert **Glc-*o*-MPN** to **o-MPN** than **Glc-*p*-MPN** to **p-MPN**.

The efficient cleavage of **Glc-*o*-MPN** and **Glc-*p*-MPN** by β-Glcase is a remarkable finding since aryl thioglycosides are known to resist the action of glucosidase enzymes. Indeed, thioglycosides are often prepared and evaluated as nonreactive glucosidase inhibitors.[40] However, substrate cleavage has been reported before when the glucoside leaving group is a thiol-substituted heterocycle with an ortho nitrogen atom.[41] This reactivity trend suggests that the pyridyl nitrogen in **Glc-*o*-MPN** and **Glc-*p*-MPN** is protonated in the β-Glcase active site, which activates C−S bond cleavage as illustrated in Scheme 2a.

Scheme 2. (a) Proposed Active Site Catalysis of Glc-*o*-MPN and Glc-*p*-MPN Cleavage by the β-Glcase Enzyme and (b) Tautomers of *o*-MPN and *p*-MPN
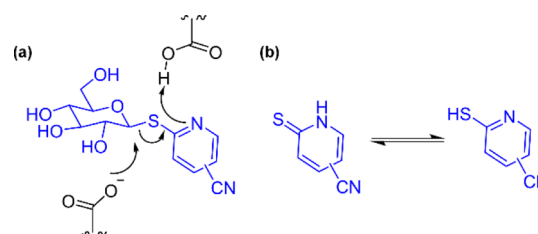
An absorption titration experiment determined the pK_a of **p-MPN** to be 6.46 (Figure S1); thus, it favors the acid form at the working pH of 5.33 used throughout this study. It is worth noting that the acidic forms of 2-mercaptopyridine compounds exist in a tautomeric equilibrium as illustrated in Scheme 2b.[42−44] The "thione" tautomer, shown on the left of the

equilibrium arrows, is the more prevalent species in aqueous solution; however, both tautomers are very likely to form the same Ag-bonded structure when *o*-MPN or *p*-MPN is captured by the surface of the AgNP as shown in Scheme 1a.[28,29]

After proving that **Glc-*o*-MPN** and **Glc-*p*-MPN** are efficient substrates for the β-Glcase enzyme, the study moved to experiments using SERS analysis. The AgNPs were prepared by standard methods, and TEM images indicated an average particle diameter of 50 nm (Figure S6). Shown in Figure 2 are
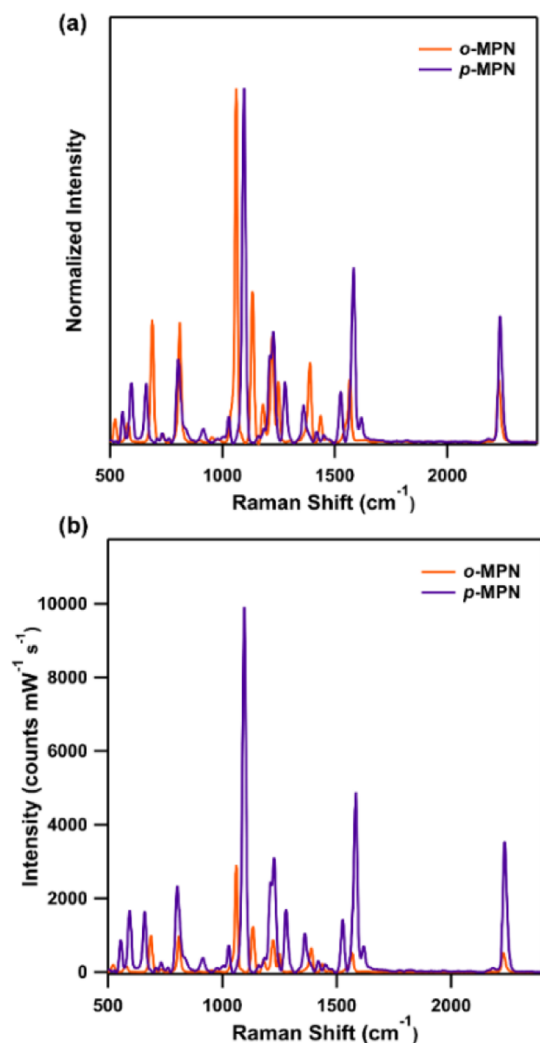

Figure 2. SERS spectra of separate samples containing equal amounts of *o*-MPN or *p*-MPN (10 μM) in the presence of preaggregated AgNPs. (a) Normalized intensity and (b) relative intensity.

SERS spectra for separate samples of *o*-MPN and *p*-MPN captured by AgNPs. The normalized spectra in Figure 2a show that both reporters produced a peak at 2230 cm^{-1}, which represents stretching of the CN bond. However, at other spectral locations, there are noticeable differences in the peak wavenumber, and especially notable are the very intense peaks at 1064 cm^{-1} for *o*-MPN and at 1096 cm^{-1} for *p*-MPN. This suggests that *o*-MPN and *p*-MPN have high potential for incorporation into multiplex detection methods that quantify the amount of each reporter in the same sample, and a demonstration of this concept is provided in Figure S11.[45,46] A comparison of the relative intensity spectra in Figure 2b shows

that *p*-MPN produces a substantially more intense spectrum than *o*-MPN, suggesting that it is likely to be a more useful reporter for a high sensitivity detection assay using a single substrate. Indeed, serial dilution experiments showed that low nanomolar concentrations of *p*-MPN can be captured by the AgNPs and easily detected at 1096 cm^{-1} (Figure 3).
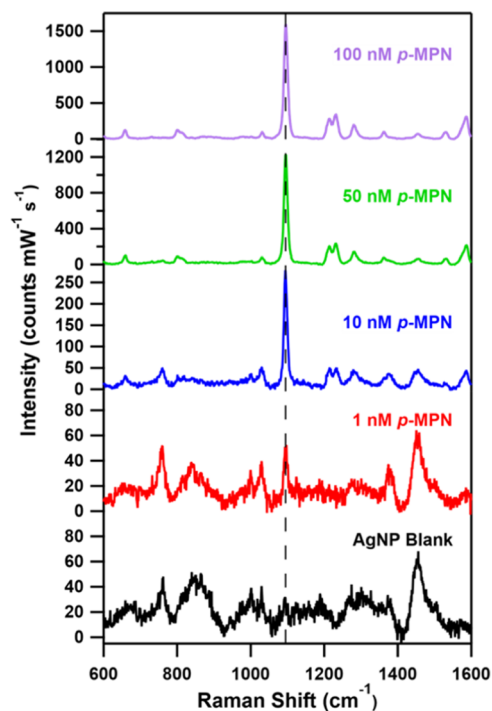

Figure 3. SERS spectra of *p*-MPN at different concentrations in the presence of AgNPs. The spectra were collected using a 633 nm laser, 1200 g/mm grating, and 120 μW power for an acquisition time of 30 s.

The greater SERS sensitivity of *p*-MPN was apparent in enzyme experiments that used AgNPs to capture the *p*-MPN or *o*-MPN that was released when **Glc-*p*-MPN** or **Glc-*o*-MPN** was cleaved by β-Glcase. The standard conditions for these enzyme experiments added an aliquot of **Glc-*o*-MPN** or **Glc-*p*-MPN** (10 μM) to a vial containing preaggregated AgNPs in PBS buffer, pH 5.33, followed by addition of β-Glcase (200 μg/mL) in the presence or absence of the CAT inhibitor (10 μg/mL). Control experiments proved that the SERS spectra for the enzyme-cleaved substrates matched the spectra for separate samples of AgNPs with added amounts of authentic *p*-MPN or *o*-MPN (Figure S7), thus confirming that the SERS spectra were reporting capture of the released SERS reporter molecules by the AgNPs. In the case of **Glc-*p*-MPN**, the intensity of the SERS spectrum before enzyme addition was very weak, and there was a large increase in signal intensity once β-Glcase had cleaved all the substrate and the AgNPs had captured all the released *p*-MPN (Figure S8a). As expected, much less *p*-MPN was produced over the standard 1 h incubation period when the assay was repeated in the presence of the inhibitor CAT (Figure S8b). The bar graph in Figure 4a shows a 20-fold increase in the SERS peak area upon complete cleavage of the substrate and substantial reduction of the peak area when β-Glcase was strongly inhibited by CAT. Similar SERS changes were also observed with **Glc-*o*-MPN** (Figure S9), but enzymatic cleavage of the substrate to release *o*-MPN
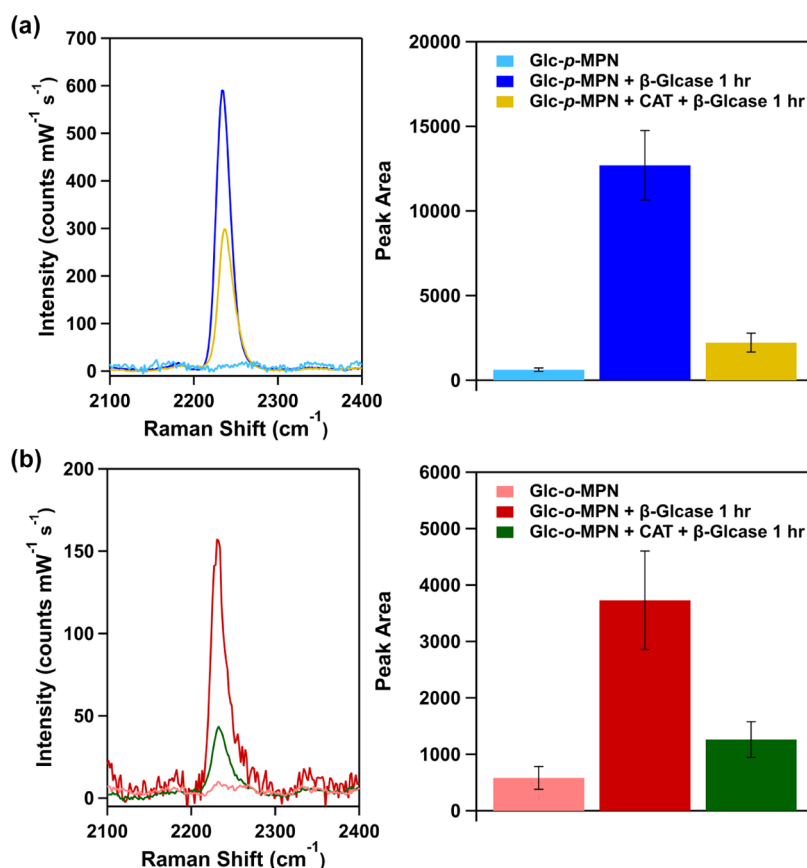
Figure 4. (a) (Left) Representative SERS spectra of 10 μM **Glc-p-MPN** after incubation for 1 h in the presence or absence of 200 μg/mL β-Glcase and 5 μg/mL CAT (1:8 molar ratio) in 1× PBS, pH 5.33, and (Right) bar graph showing the average peak area at 2230 cm^{-1}. (b) (Left) Representative SERS spectra of 10 μM **Glc-o-MPN** after incubation for 1 h in the presence or absence of 200 μg/mL β-Glcase and 5 μg/mL CAT in 1× PBS, pH 5.33, and (Right) bar graph (N = 3) showing the average peak area at 2230 cm^{-1}. The peak area has units of counts mW^{-1} s^{-1} cm^{-1}.
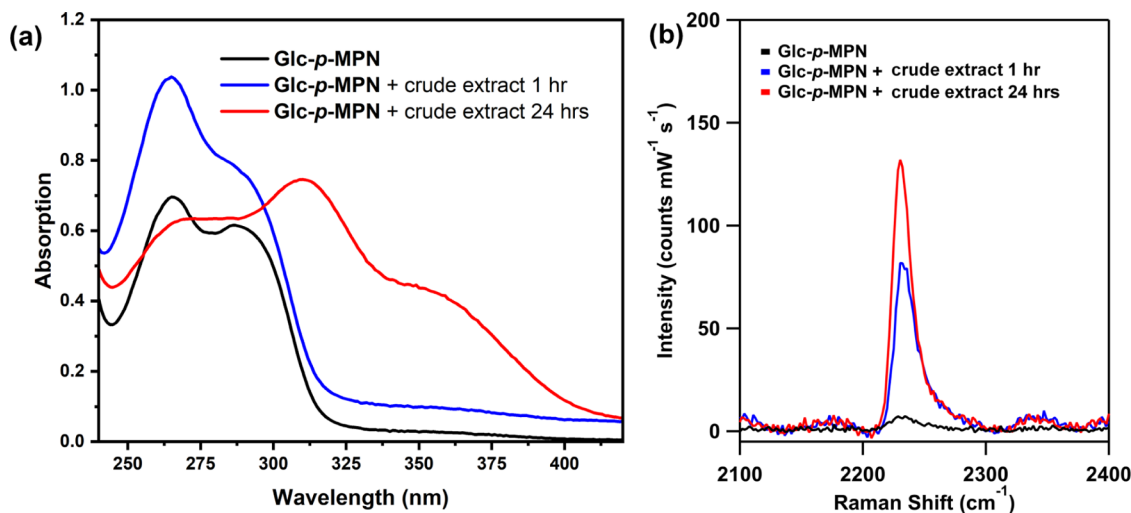

Figure 5. (a) Representative UV−vis spectra of 50 μM **Glc-p-MPN** before and after 1 h or after 24 h of incubation with crude almond flour extract (protein concentration of 200 μg/mL). (b) Representative SERS spectra of 10 μM **Glc-p-MPN** before and after 1 h or after 24 h of incubation with a crude almond flour extract (protein concentration of 200 μg/mL). In all cases, the assay solution was 1× PBS, pH 5.33.

as the reporter molecule only produced a sixfold increase in the CN peak area at 2230 cm^{-1} (Figure 4b).

The selectivity of this SERS-based enzyme assay was tested by conducting a set of experiments that mixed separate samples of **Glc-p-MPN** with high amounts of other analytes that might have affinity for the AgNPs and thus possibly produce an

artifact (i.e., bovine serum albumin, cysteine, glutathione, glycine, or lipase).[47] As shown in Figure S10, only β-Glcase produced a large SERS signal corresponding to released **p-MPN**. Additional experiments proved that the SERS-based assay worked equally well with preaggregated AuNPs (Figure S13).

The corollary of the high sensitivity gained by SERS detection is the possibility of diagnostic tests that can detect enzyme activities in a much shorter time period compared to detection by UV−vis absorption. We tested this idea by performing an experiment that compared the relative capabilities of the SERS and UV−vis detection methods to report positive evidence for cleavage of **Glc-*p*-MPN** by *β*-Glcase. The comparative experiment employed a sample of crude almond flour extract and mimicked a real-world circumstance, namely quality control screening of a food source for evidence that it contains a desired threshold level of flavor-enhancing *β*-Glcase activity.[32−34] Since the *β*-Glcase activity in a typical crude almond flour extract is quite low, a practically useful diagnostic test needs to detect the appearance of *p*-MPN with high sensitivity.

Two separate samples from the same stock solution of crude almond extract were tested for capacity to cleave **Glc-*p*-MPN** and produce *p*-MPN (*β*-Glcase activity). One sample was assessed by UV−vis, and the other was assessed by SERS. In both cases, the spectrum for a solution of **Glc-*p*-MPN** was acquired before extract addition and again at 1 or 24 h after the addition of the crude almond extract (protein concentration of 200 μg/mL). Inspection of the UV−vis spectra in Figure 5a shows that appearance of the *p*-MPN band at 312 nm (or 360 nm) was not very clear after 1 h but was quite apparent after 24 h, with both spectra exhibiting significant background absorption at <300 nm due to other proteins present in the crude extract. In contrast, the SERS spectra in Figure 5b show that appearance of the *p*-MPN peak 2230 cm^{-1} was very apparent after 1 h with no evidence of any background SERS signal due to other proteins. The results clearly show that the presence of *β*-glucosidase activity in the crude almond extract is confirmed by SERS detection in a much shorter time period (>10 times shorter) than by UV−vis absorption detection. Obviously, this substantial time saving would greatly facilitate any industrial food production process that must perform a large number of quality assurance measurements to confirm the threshold levels of *β*-glucosidase activity.

Close inspection of the SERS data in Figures 3 and 5 suggests that dependence of the SERS signal intensity on the *p*-MPN concentration is not perfectly linear, which we attribute to the use of preaggregated nanoparticles for the SERS measurements. Thus, future work to optimize the assays will need to develop a suitable immobilized metal surface for SERS detection, in particular a surface with a more uniform and reproducible morphology that enables improved quantitative analysis. This is an ongoing community-wide research challenge that must be solved before SERS-based assays will be routinely used for quantitative enzyme detection.[25,48,49]

CONCLUSIONS

The two 2-mercaptopydrine-carbonitrile compounds, *o*-MPN or *p*-MPN, have great potential as reporter molecules for efficient capture by silver or AuNPs and detection by SERS. The specific focus of this study was on enzyme sensing, and the results show that **Glc-*p*-MPN** and **Glc-*o*-MPN** are efficient substrates for the *β*-Glcase enzyme, which enable SERS detection of *β*-Glcase activity and *β*-Glcase inhibition. The substrate **Glc-*p*-MPN** is superior because the released *p*-MPN is detected with higher sensitivity. Comparative sensitivity experiments using an almond flour extract showed that the presence of *β*-glucosidase activity in the crude extract could be confirmed by SERS detection in a much shorter time period

(>10 times shorter) than by UV−vis absorption detection. With further development, it is possible that *β*-Glcase assays using **Glc-*p*-MPN** will be broadly useful in environmental science[31] and disease diagnosis.[35,36] SERS detection will be especially helpful with heterogeneous samples such as saliva[50] or bacterial cell culture,[33] where optical assays fail due to strong scattering of light and background interference.

Beyond the specific application of *β*-Glcase sensing, it is very likely that many other enzyme assays can be developed using released 2-mercaptopydrine-carbonitriles as SERS reporter molecules. In addition to single-use assays, it should be possible to spatially pattern the AgNP capture agent in an array format that enables high-throughput screening of enzyme inhibitors for drug discovery.[8,48] Alternatively, enzyme−antibody conjugates can be developed for enzyme-catalyzed signal amplification with SERS detection in ELISA-based diagnostics.[51] The narrow peaks and high signal dispersion of SERS spectra favor multiplex diagnostics and imaging, which raises the possibility of additional 2-mercaptopydrine-carbonitrile compounds, beyond *o*-MPN and *p*-MPN, as reporter molecules with distinct spectral SERS signals that can act as detection barcodes.[52]

■ ASSOCIATED CONTENT

Ⓢ Supporting Information

The Supporting Information is available free of charge at https://pubs.acs.org/doi/10.1021/acsomega.2c00139.

> Synthetic methods and compound characterization, enzyme kinetic characterization, comparison of Michaelis−Menten parameters, supplementary spectral data for enzyme assays, TEM micrographs of AgNPs and AuNPs, supplementary SERS spectra, and protein quantification data (PDF)

■ AUTHOR INFORMATION

Corresponding Authors

Jon P. Camden − *Department of Chemistry and Biochemistry, University of Notre Dame, Notre Dame, Indiana 46556-5670, Unites States;* ⓘ orcid.org/0000-0002-6179-2692; Email: jcamden3@nd.edu

Bradley D. Smith − *Department of Chemistry and Biochemistry, University of Notre Dame, Notre Dame, Indiana 46556-5670, Unites States;* ⓘ orcid.org/0000-0003-4120-3210; Email: smith.115@nd.edu

Authors

Janeala J. Morsby − *Department of Chemistry and Biochemistry, University of Notre Dame, Notre Dame, Indiana 46556-5670, Unites States;* ⓘ orcid.org/0000-0002-0700-5969

Rebekah L. Thimes − *Department of Chemistry and Biochemistry, University of Notre Dame, Notre Dame, Indiana 46556-5670, Unites States;* ⓘ orcid.org/0000-0001-6333-126X

Jacob E. Olson − *Department of Chemistry and Biochemistry, University of Notre Dame, Notre Dame, Indiana 46556-5670, Unites States;* ⓘ orcid.org/0000-0001-7110-1739

Hannah H. McGarraugh − *Department of Chemistry and Biochemistry, University of Notre Dame, Notre Dame, Indiana 46556-5670, Unites States*

Jason N. Payne − *Department of Chemistry and Biochemistry, University of Notre Dame, Notre Dame, Indiana 46556-5670, Unites States;* ● orcid.org/0000-0002-2549-1665

Complete contact information is available at:
https://pubs.acs.org/10.1021/acsomega.2c00139

Author Contributions

H.H.M. and J.N.P. synthesized the compounds. J.J.M. conducted the enzyme kinetic experiments. J.J.M., R.L.T., and J.E.O. conducted the SERS experiments. J.P.C. and B.D.S. supervised the project. The article was written through contributions of all authors. All authors have given approval to the final version of the article.

Notes

The authors declare no competing financial interest.

■ REFERENCES

(1) Seitkalieva, A. V.; Menzorova, N. I.; Rasskazov, V. A. Application of Different Enzyme Assays and Biomarkers for Pollution Monitoring of the Marine Environment. *Environ. Monit. Assess.* **2016**, *188*, 70.

(2) Holdgate, G. A.; Meek, T. D.; Grimley, R. L. Mechanistic Enzymology in Drug Discovery: A Fresh Perspective. *Nat. Rev. Drug Discovery* **2018**, *17*, 115−132.

(3) Carter, L. J.; Garner, L. V.; Smoot, J. W.; Li, Y.; Zhou, Q.; Saveson, C. J.; Sasso, J. M.; Gregg, A. C.; Soares, D. J.; Beskid, T. R.; et al. Assay Techniques and Test Development for COVID-19 Diagnosis. *ACS Cent. Sci.* **2020**, *6*, 591−605.

(4) Miyamoto, S.; Sano, S.; Takahashi, K.; Jikihara, T. Method for Colorimetric Detection of Double-Stranded Nucleic Acid Using Leuco Triphenylmethane Dyes. *Anal. Biochem.* **2015**, *473*, 28−33.

(5) Reetz, M. T.; Houben-weyl, C.; Doyle, M. P.; Dorow, R. L.; Buhro, W. E.; Griffin, J. H.; Liebeton, K.; Jaeger, K. Creation of Enantioselective Biocatalysts for Organic Chemistry by In Vitro Evolution. *Angew. Chem., Int. Ed.* **1997**, *36*, 2830−2832.

(6) Akhtar, M. K.; Vijay, D.; Umbreen, S.; McLean, C. J.; Cai, Y.; Campopiano, D. J.; Loake, G. J. Hydrogen Peroxide-Based Fluorometric Assay for Real-Time Monitoring of SAM-Dependent Methyltransferases. *Front. Bioeng. Biotechnol.* **2018**, *6*, 146.

(7) Gabr, M. T.; Pigge, F. C. Expanding the Toolbox for Label-Free Enzyme Assays: A Dinuclear Platinum(II) Complex/DNA Ensemble with Switchable Near-IR Emission. *Molecules* **2019**, *24*, 4390.

(8) Acker, M. G.; Auld, D. S. Considerations for the Design and Reporting of Enzyme Assays in High-Throughput Screening Applications. *Perspect. Sci.* **2014**, *1*, 56−73.

(9) Ma, L.; Zhang, Z.; Li, X. Non-Invasive Disease Diagnosis Using Surface-Enhanced Raman Spectroscopy of Urine and Saliva. *Appl. Spectrosc. Rev.* **2020**, *55*, 197−219.

(10) Mohapatra, H.; Phillips, S. T. Reagents and Assay Strategies for Quantifying Active Enzyme Analytes Using a Personal Glucose Meter. *Chem. Commun.* **2013**, *49*, 6134−6136.

(11) Torrini, F.; Palladino, P.; Brittoli, A.; Baldoneschi, V.; Minunni, M.; Scarano, S. Characterization of Troponin T Binding Aptamers for an Innovative Enzyme-Linked Oligonucleotide Assay (ELONA). *Anal. Bioanal. Chem.* **2019**, *411*, 7709−7716.

(12) Kim, Y.-P.; Kim, H.-S. Nanoparticles for Use in Enzyme Assays. *ChemBioChem* **2016**, *17*, 275−282.

(13) Li, Z.; Leustean, L.; Inci, F.; Zheng, M.; Demirci, U.; Wang, S. Plasmonic-Based Platforms for Diagnosis of Infectious Diseases at the Point-of-Care. *Biotechnol. Adv.* **2019**, *37*, 107440.

(14) Tokel, O.; Inci, F.; Demirci, U. Advances in Plasmonic Technologies for Point of Care Applications. *Chem. Rev.* **2014**, *114*, 5728−5752.

(15) Dos Santos, D. P.; Andrade, G. F. S.; Temperini, M. L. A.; Brolo, A. G. Electrochemical Control of the Time-Dependent Intensity Fluctuations in Surface-Enhanced Raman Scattering (SERS). *J. Phys. Chem. C* **2009**, *113*, 17737−17744.

(16) Bi, L.; Wang, Y.; Yang, Y.; Li, Y.; Mo, S.; Zheng, Q.; Chen, L. Highly Sensitive and Reproducible SERS Sensor for Biological PH Detection Based on a Uniform Gold Nanorod Array Platform. *ACS Appl. Mater. Interfaces* **2018**, *10*, 15381−15387.

(17) Larmour, I. A.; Faulds, K.; Graham, D. The Past, Present and Future of Enzyme Measurements Using Surface Enhanced Raman Spectroscopy. *Chem. Sci.* **2010**, *1*, 151−160.

(18) Leopold, N.; Lendl, B. A New Method for Fast Preparation of Highly Surface-Enhanced Raman Scattering (SERS) Active Silver Colloids at Room Temperature by Reduction of Silver Nitrate with Hydroxylamine Hydrochloride. *J. Phys. Chem. B* **2003**, *107*, 5723−5727.

(19) Rodger, C.; Smith, W. E.; Dent, G.; Edmondson, M. Surface-Enhanced Resonance-Raman Scattering: An Informative Probe of Surfaces. *J. Chem. Soc., Dalton Trans.* **1996**, *1*, 791−799.

(20) Vo-Dinh, T.; Houck, K.; Stokes, D. L. Surface-Enhanced Raman Gene Probes. *Anal. Chem.* **1994**, *66*, 3379−3383.

(21) Moore, B. D.; Stevenson, L.; Watt, A.; Flitsch, S.; Turner, N. J.; Cassidy, C.; Graham, D. Rapid and Ultra-Sensitive Determination of Enzyme Activities Using Surface-Enhanced Resonance Raman Scattering. *Nat. Biotechnol.* **2004**, *22*, 1133−1138.

(22) Yu, Z.; Chen, L.; Wang, Y.; Wang, X.; Song, W.; Ruan, W.; Zhao, B.; Cong, Q. A SERS-Active Enzymatic Product Used for the Quantification of Disease-Related Molecules. *J. Raman Spectrosc.* **2014**, *45*, 75−81.

(23) Gu, X.; Trujillo, M. J.; Olson, J. E.; Camden, J. P. SERS Sensors: Recent Developments and a Generalized Classification Scheme Based on the Signal Origin. *Annu. Rev. Anal. Chem.* **2018**, *11*, 147−169.

(24) Soualmia, F.; Touhar, S. A.; Guo, L.; Xu, Q.; Garland, M.; Percot, A.; El Amri, C.; El Amri, C. Amino-Methyl Coumarin as a Potential SERS@Ag Probe for the Evaluation of Protease Activity and Inhibition. *J. Raman Spectrosc.* **2017**, *48*, 82−88.

(25) Nirala, N. R.; Asiku, J.; Dvir, H.; Shtenberg, G. N-Acetyl-β-D-Glucosaminidase Activity Assay for Monitoring Insulin-Dependent Diabetes Using Ag-Porous Si SERS Platform. *Talanta* **2022**, *239*, 123087.

(26) Yuan, H.; Ji, W.; Chu, S.; Liu, Q.; Qian, S.; Guang, J.; Wang, J.; Han, X.; Masson, J.-F.; Peng, W. Mercaptopyridine-Functionalized Gold Nanoparticles for Fiber-Optic Surface Plasmon Resonance Hg^{2+} Sensing. *ACS Sens.* **2019**, *4*, 704−710.

(27) Chen, L.; Fu, X.; Li, J. Ultrasensitive Surface-Enhanced Raman Scattering Detection of Trypsin Based on Anti-Aggregation of 4-Mercaptopyridine-Functionalized Silver Nanoparticles: An Optical Sensing Platform toward Proteases. *Nanoscale* **2013**, *5*, 5905−5911.

(28) Singh, P.; Deckert-Gaudig, T.; Zhang, Z.; Deckert, V. Plasmon Induced Deprotonation of 2-Mercaptopyridine. *Analyst* **2020**, *145*, 2106−2110.

(29) Nunes, F. S.; Bonifácio, L. D. S.; Araki, K.; Toma, H. E. Interaction of 2- and 4-Mercaptopyridine with Pentacyanoferrates and Gold Nanoparticles. *Inorg. Chem.* **2006**, *45*, 94−101.

(30) Das, S. K.; Bhattacharya, T. S.; Ghosh, M.; Chowdhury, J. Probing Blood Plasma Samples for the Detection of Diabetes Using SERS Aided by PCA and LDA Multivariate Data Analyses. *New J. Chem.* **2021**, *45*, 2670−2682.

(31) Singh, G.; Verma, A. K.; Kumar, V. Catalytic Properties, Functional Attributes and Industrial Applications of β-Glucosidases. *3 Biotech* **2016**, *6*, 3−14.

(32) Singhania, R. R.; Patel, A. K.; Sukumaran, R. K.; Larroche, C.; Pandey, A. Role and Significance of Beta-Glucosidases in the Hydrolysis of Cellulose for Bioethanol Production. *Bioresour. Technol.* **2013**, *127*, 500−507.

(33) Strahsburger, E.; de Lacey, A. M. L.; Marotti, I.; DiGioia, D.; Biavati, B.; Dinelli, G. In Vivo Assay to Identify Bacteria with β-Glucosidase Activity. *Electron. J. Biotechnol.* **2017**, *30*, 83−87.

(34) Srivastava, N.; Rathour, R.; Jha, S.; Pandey, K.; Srivastava, M.; Thakur, V. K.; Sengar, R. S.; Gupta, V. K.; Mazumder, P. B.; Khan, A. F.; et al. Microbial Beta Glucosidase Enzymes: Recent Advances in Biomass Conversation for Biofuels Application. *Biomolecules* **2019**, *9*, 220.

(35) Fateen, E.; Abdallah, Z. Y. Twenty- Five Years of Biochemical Diagnosis of Gaucher Disease: The Egyptian Experience. *Heliyon* **2019**, *5*, No. e02574.

(36) Jin, M.-Y.; Zhang, T.; Yang, Y.-S.; Ding, Y.; Li, J.-S.; Zhong, G.-R. A Simplified and Miniaturized Glucometer-Based Assay for the Detection of β-Glucosidase Activity. *J. Zhejiang Univ., Sci., B* **2019**, *20*, 264−272.

(37) Lee, P. C.; Meisel, D. Adsorption and Surface-Enhanced Raman of Dyes on Silver and Gold Sols. *J. Phys. Chem.* **1982**, *86*, 3391−3395.

(38) Frens, G.; Kolloid, Z. Controlled Nucleation for the Regulation of the Particle Size in Monodisperse Gold Suspensions. *Nat. Phys. Sci.* **1973**, *241*, 20.

(39) Yu, H.-L.; Xu, J.-H.; Lu, W.-Y.; Lin, G.-Q. Identification, Purification and Characterization of β-Glucosidase from Apple Seed as a Novel Catalyst for Synthesis of O-Glucosides. *Enzyme Microb. Technol.* **2007**, *40*, 354−361.

(40) Samoshin, A. V.; Dotsenko, I. A.; Samoshina, N. M.; Franz, A. H.; Samoshin, V. V. Thio- β -D-Glucosides: Synthesis and Evaluation as Glycosidase Inhibitors and Activators. *Int. J. Carbohydr. Chem.* **2014**, *2014*, 941059.

(41) Avegno, E. A.-B.; Hasty, S. J.; Parameswar, A. R.; Howarth, G. S.; Demchenko, A. V.; Byers, L. D. Reactive Thioglucoside Substrates for β-Glucosidase. *Arch. Biochem. Biophys.* **2013**, *537*, 1−4.

(42) Bomzon, B.; Khunger, Y.; Subramanian, R. A Dielectric and Spectrophotometric Study of the Tautomerization of 2-Hydroxypyridine and 2-Mercaptopyridine in Water. *RSC Adv.* **2020**, *10*, 2389−2395.

(43) Stoyanov, S.; Petkov, I.; Antonov, L.; Stoyanova, T.; Karagiannidis, P.; Aslanidis, P. Thione-Thiol Tautomerism and Stability of 2- and 4-Mercaptopyridines and 2-Mercaptopyridines. *Can. J. Chem.* **1990**, *68*, 1482−1489.

(44) Pang, Y. S.; Hwang, H. J.; Kim, M. S. Adsorption of 2-Mercaptopyridine and 2-Mercaptopyrimidine on a Silver Colloidal Surface Investigated by Raman Spectroscopy. *J. Mol. Struct.* **1998**, *441*, 63−76.

(45) Huang, R.; Harmsen, S.; Samii, J. M.; Karabeber, H.; Pitter, K. L.; Holland, E. C.; Kircher, M. F. High Precision Imaging of Microscopic Spread of Glioblastoma with a Targeted Ultrasensitive SERRS Molecular Imaging Probe. *Theranostics* **2016**, *6*, 1075−1084.

(46) Oseledchyk, A.; Andreou, C.; Wall, M. A.; Kircher, M. F. Folate-Targeted Surface-Enhanced Resonance Raman Scattering Nanoprobe Ratiometry for Detection of Microscopic Ovarian Cancer. *ACS Nano* **2017**, *11*, 1488−1497.

(47) Li, J.; Chen, L.; Lou, T.; Wang, Y. Highly Sensitive SERS Detection of As3+ Ions in Aqueous Media Using Glutathione Functionalized Silver Nanoparticles. *ACS Appl. Mater. Interfaces* **2011**, *3*, 3936−3941.

(48) Zhang, M.; Jin, C.; Nie, Y.; Ren, Y.; Hao, N.; Xu, Z.; Dong, L.; Zhang, J. X. J. Silver Nanoparticle on Zinc Oxide Array for Label-Free Detection of Opioids through Surface-Enhanced Raman Spectroscopy. *RSC Adv.* **2021**, *11*, 11329−11337.

(49) Mu, T.; Wang, S.; Li, T.; Wang, B.; Ma, X.; Huang, B.; Zhu, L.; Guo, J. Detection of Pesticide Residues Using Nano-SERS Chip and a Smartphone-Based Raman Sensor. *IEEE J. Sel. Top. Quantum Electron.* **2018**, *25*, 5200206.

(50) Stradwick, L.; Inglis, D.; Kelly, J.; Pickering, G. Development and Application of Assay for Determining β-Glucosidase Activity in Human Saliva. *Flavour* **2017**, *6*, 1−8.

(51) Zhang, Y.; Mi, X.; Tan, X.; Xiang, R. Recent Progress on Liquid Biopsy Analysis Using Surface-Enhanced Raman Spectroscopy. *Theranostics* **2019**, *9*, 491−525.

(52) Hu, F.; Zeng, C.; Long, R.; Miao, Y.; Wei, L.; Xu, Q.; Min, W. Supermultiplexed Optical Imaging and Barcoding with Engineered Polyynes. *Nat. Methods* **2018**, *15*, 194−200.